Available online at www.sciencedirect.com
ScienceDirect
Polymer 48 (2007) 2130–2143
polymer
www.elsevier.com/locate/polymer

Effects of internal linkage groups of fluorinated diamine on the optical and dielectric properties of polyimide thin films

Wonbong Jang [a], Daeyong Shin [a], Seunghyuk Choi [a], Sunggook Park [b], Haksoo Han [a,*]

[a] Department of Chemical Engineering, Yonsei University, 134 Shinchon-dong, Sedaemun-gu, Seoul 120-749, Republic of Korea
[b] Department of Mechanical Engineering, Louisiana State University, 2212A CEBA Building, Baton Rouge, LA 70803-6413, United States

Received 16 October 2006; received in revised form 16 January 2007; accepted 11 February 2007
Available online 14 February 2007

Abstract

To investigate the difference of the trifluoromethyl (CF_3) group and ether group affecting the optical property of fluorinated polyimides (PIs), we prepared 4,4′-bis(4-amino-2-trifluoromethylphenoxy)diphenyl ether (**4**) with three ether groups and 2,2-bis[4-(4-amino-2-trifluoromethylphenoxy)phenyl]hexafluoropropane (**5**) with four CF_3 groups with 2-chloro-5-nitrobenzotrifluoride and 4,4′-dihydroxydiphenyl ether or 2,2-bis(4-hydroxyphenol)hexafluoropropane. Two series of organosoluble and light-colored PIs (**4a–4c**, **5a–5c**) were synthesized from **4** and **5** with various aromatic dianhydrides: 3,3,4,4-benzophenonetetracarboxylic dianhydride (BTDA) (**a**), 4,4-oxydiphthalic anhydride (ODPA) (**b**), and 4,4-hexafluoroisopropylidenediphthalic anhydride (6FDA) (**c**), prepared through a typical two-step polymerization method. These PIs were soluble in amide polar solvents and even in less polar solvents. The glass-transition temperatures (T_g) of **4a–5c** were 221–249 °C and the 10% weight-loss temperatures were above 530 °C. Their films had cutoff wavelengths between 339 and 399 nm and yellowness index ranges from 1.95 to 42.60. The dielectric constants estimated from the average refractive indices are 2.59–2.93 (1 MHz). In a comparison of the PI series based on **4**, **5**, and 4,4′-bis(4-amino-2-trifluoromethylphenoxy)biphenyl (**6**), we found that the CF_3 group and ether group on the diamine had almost same effect in lowering the color, but the ether group had better thermal stability. The color intensity of the three PI series was lowered in the following order: **6** > **4** > **5**. The PI **5c**, synthesized from diamine **5** and dianhydride **c**, had six CF_3 groups in a repeated segment and ether group at the same time, so it exhibited the lightest color among the three series.

Keywords: Fluorine-containing polyimides; Solubility; Color intensity

1. Introduction

Aromatic polyimides (PIs) are well known as a class of high-performance polymers because of their outstanding properties, such as high thermal stability, high mechanical performance, good chemical resistance, and excellent electrical properties. These materials are widely used in the aerospace and electronic industries [1]. Depending on the application, optical transparency of PI films is of special importance, such as flexible solar radiation protectors [2], orientation films in liquid crystal display devices [3] and optical half-wave plates for planar lightwave circuits [4]. However, most PIs between UV and the visible area have strong absorption, rendering their color close to yellow or brown because of their highly conjugated aromatic structures and the intermolecular charge-transfer complex (CTC) formation. In addition, most PIs are insoluble and infusible in their fully imidized form because of their rigid chain structure. Thus, their processing is generally completed at the poly(amic acid) stage, which would prevent their use in some applications. To improve their processability, numerous research efforts have been focused on the synthesis of soluble and melt-processable PIs that retain their thermal stability and other excellent properties [5–7]. Therefore, great efforts have been expended to develop advanced PI material with both good solubility and transparency.

The solubilization of rigid-chain polymers has been made through the synthetic modification of the flexibilizing linkages

* Corresponding author. Tel.: +82 2 2123 2764; fax: +82 2 312 6401.
E-mail address: hshan@yonsei.ac.kr (H. Han).

0032-3861/$ - see front matter © 2007 Elsevier Ltd. All rights reserved.
doi:10.1016/j.polymer.2007.02.023

[8,9] or by introducing bulky side group [10,11] or molecular asymmetry (*ortho*, *meta* versus linkages) [12,13] into the backbone. The main concepts indicated all of these approaches in the introduction of several types of polymer chain–chain interactions, chain packing, and charge-transfer electronic polarization interactions.

To increase the optical applications of PIs, a number of very lightly colored to colorless, transparent PI films have been synthesized and characterized. It has been also proved that PI with trifluoromethyl (CF_3) or the ether group can enhance the solubility and thermal stability, reduce dielectric constant and moisture absorption and raise the optical transparency [13,14]. Rogers first reported that optically transparent and colorless PIs could be synthesized from a dianhydride and a diamine with hexafluoroisopropylidene ($-C(CF_3)_2-$) groups [15]. Dine-Hart and Wright showed the formation of CTC between alternating electron-donor (diamine) and electron-acceptor (dianhydride) moieties [16]. Also, the introduction of kink structures, like ether group, into polymer chains might prevent their alignment and so disrupt effective CTC formation. These studies could result in valuable applications, such as the formation of colorless polymer films with high transmittance [17].

In this study, a highly kinked diamine, 4,4′-bis(4-amino-2-trifluoromethylphenoxy)diphenyl ether (**4**), and a highly fluorinated diamine, 2,2-bis[4-(4-amino-2-trifluoromethylphenoxy)phenyl]hexafluoropropane (**5**), were synthesized and subsequently poly-condensed with various commercially available aromatic dianhydrides to produce two series of fluorinated PIs (**4a–4c**, **5a–5c**). Although **5** and its polymer were reported by Wang and Yang [18] and Liaw and Chang [19], their results were different from ours and they showed only the effects of diamine with fluorinated groups on the color lightness. They failed to investigate the difference of the CF_3 group and ether group affecting the optical property of PIs. To investigate the difference of the CF_3 group and ether group affecting the color intensity and optical transparency of PIs, we prepared and characterized the PI series **4** (with three ether groups), series **5** (with four CF_3 groups) and series **6** (without CF_3 group and ether group in the center of diamine chain). We synthesized diamine **4** and then discussed about the optical properties, solubility, dielectric constant and thermal properties of **4a–4c**, we also compared it with the PI series **5a–5c** and **6a–6c**, which were based on **5** and 4,4′-bis(4-amino-2-trifluoromethylphenoxy)-biphenyl (**6**), to investigate the point of difference between the ether group and the CF_3 group affecting coloration, respectively.

2. Experimental

2.1. Materials

2-Chloro-5-nitrobenzotrifluoride (Aldrich), 4,4′-dihydroxydiphenyl ether (TCI), 4,4′-dihydroxydiphenyl (TCI) and 2,2-bis(4-hydroxyphenol)hexafluoropropane (TCI) were used as received. The aromatic dianhydrides, 3,3,4,4-benzophenonetetracarboxylic dianhydride (BTDA; TCI) and 4,4-oxydiphthalic anhydride (ODPA; Aldrich) were recrystallized from acetic anhydride before use. 4,4-Hexafluoroisopropylidenediphthalic anhydride (6FDA; TCI) was purified by sublimation. *N*,*N*-dimethylacetamide (DMAc; Aldrich) and pyridine (Py; Wako) were purified by distillation under reduced pressure over calcium hydride and stored over 4-Å molecular sieves.

2.2. Monomer synthesis

2.2.1. 4,4′-Bis(4-nitro-2-trifluoromethylphenoxy)diphenyl ether (*1*)

4,4′-Dihydroxydiphenyl ether (0.02 mol) and 2-chloro-5-nitrobenzotrifluoride (0.04 mol) were first dissolved with DMAc in a three-neck round bottom flask with stirring. After the mixture was completely dissolved, potassium carbonate was added to it. After 30 min of stirring at room temperature, the mixture was heated at 110 °C for 24 h. The obtained mixture was poured into water to give solid, which was collected and washed with water. Then, the solid was dried in vacuum at 80 °C for 10 h. The crude product was recrystallized from ethanol to give fine, lightly yellow needle-like crystals of **1** (11.23 g, yield: 88.1%).

The melting point (T_m) is 192 °C by differential scanning calorimetry (DSC) at a scan rate of 10 °C/min. IR (KBr): 1529, 1334 ($-NO_2$ stretch), 1238 (C–F stretch), 1186, 1139 cm^{-1} (C–O stretch) (Fig. 1). ^1H NMR [500 MHz, dimethyl sulfoxide

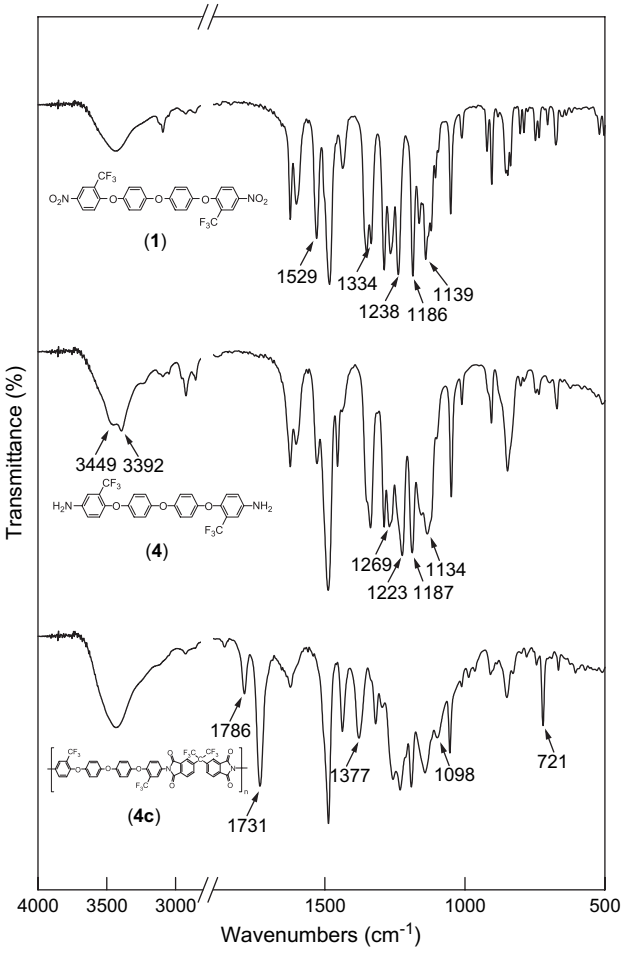

Fig. 1. FTIR spectra of nitro compound (**1**), diamine (**4**), and polyimide (**4c**).

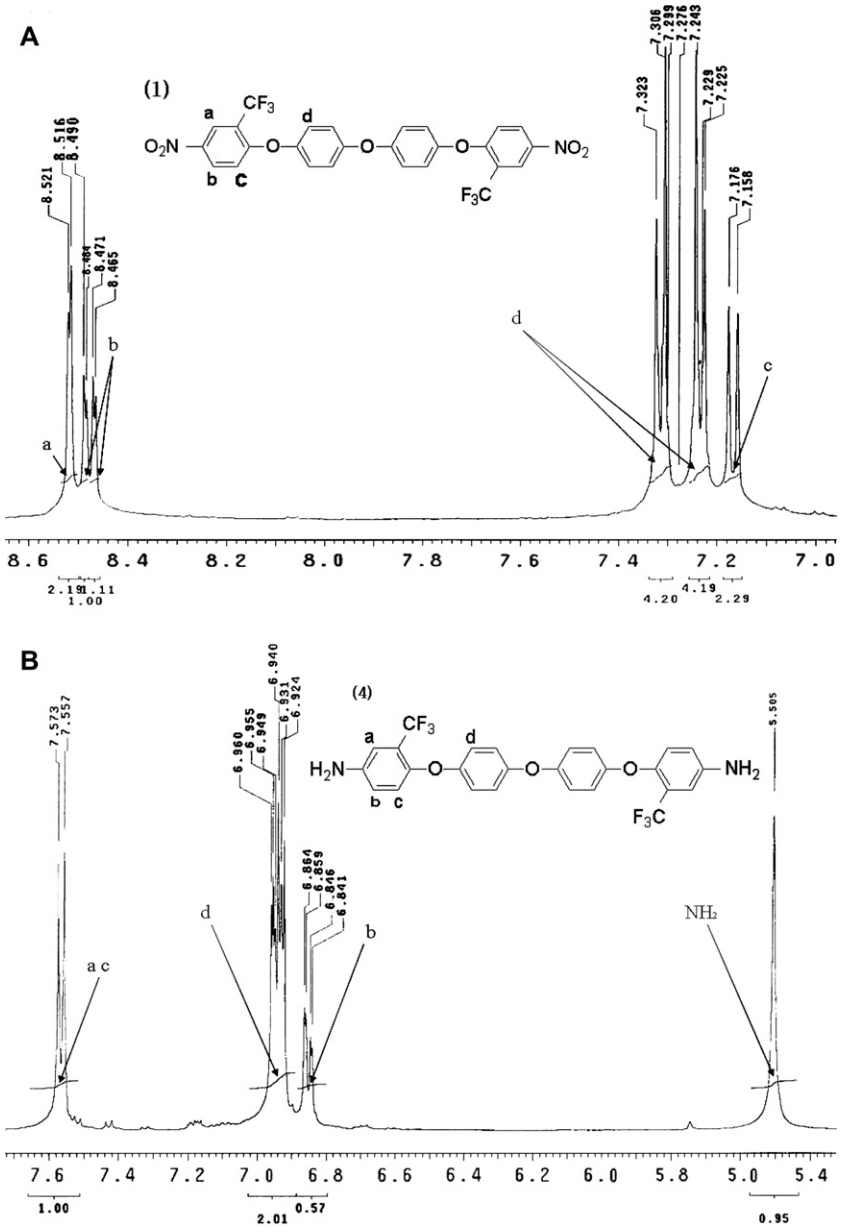

Fig. 2. ^{1}H NMR spectra of (A) dinitro compound (**1**) and (B) diamine (**4**).

(DMSO)]: δ (ppm) 8.521, 8.516 (2H, H_a), 8.490–8.465 (2H, H_b), 7.323–7.225 (8H, H_d), 7.176, 7.158 (2H, H_c) (Fig. 2).

2.2.2. 2,2-Bis[4-(4-nitro-2-trifluoromethylphenoxy)phenyl]-hexafluoropropane (*2*)

2,2-Bis(4-hydroxyphenol)hexafluoropropane (0.02 mol) and 2-chloro-5-nitrobenzotrifluoride (0.04 mol) were first dissolved with DMAc in a three-neck round bottom flask with stirring. After the mixture was completely dissolved, potassium carbonate was added to it. After 30 min of stirring at room temperature, the mixture was heated at 110 °C for 24 h. The obtained mixture was poured into water to give solid, which was collected and washed with water. Then, the solid was dried in vacuum at 80 °C for 10 h. The crude product was recrystallized from ethanol to give fine, lightly yellow needle-like crystals of **2** (12.35 g, yield: 86.4%).

The T_m is 184 °C by differential scanning calorimetry (DSC) at a scan rate of 10 °C/min. IR (KBr): 1538, 1331 (−NO_2 stretch), 1265 (C−F stretch), 1172, 1130 cm^{-1} (C−O stretch). ^{1}H NMR (500 MHz, DMSO): δ (ppm) 8.557, 8.552 (2H, H_a), 8.532–8.508 (2H, H_b), 7.43, 7.525 (4H, H_e), 7.398, 7.380 (4H, H_d), 7.334, 7.315 (2H, H_c) (Fig. 3).

2.2.3. 4,4′-Bis(4-nitro-2-trifluoromethylphenoxy)-diphenyl (*3*)

Similarly, **3** (10.27 g, yield: 91%) was prepared with the aforementioned procedure.

The T_m is 224 °C by differential scanning calorimetry (DSC) at a scan rate of 10 °C/min. IR (KBr): 1528, 1333 (−NO_2 stretch), 1275 (C−F stretch), 1152, 1124 cm^{-1} (C−O stretch). ^{1}H NMR (500 MHz, DMSO): δ (ppm) 8.532,

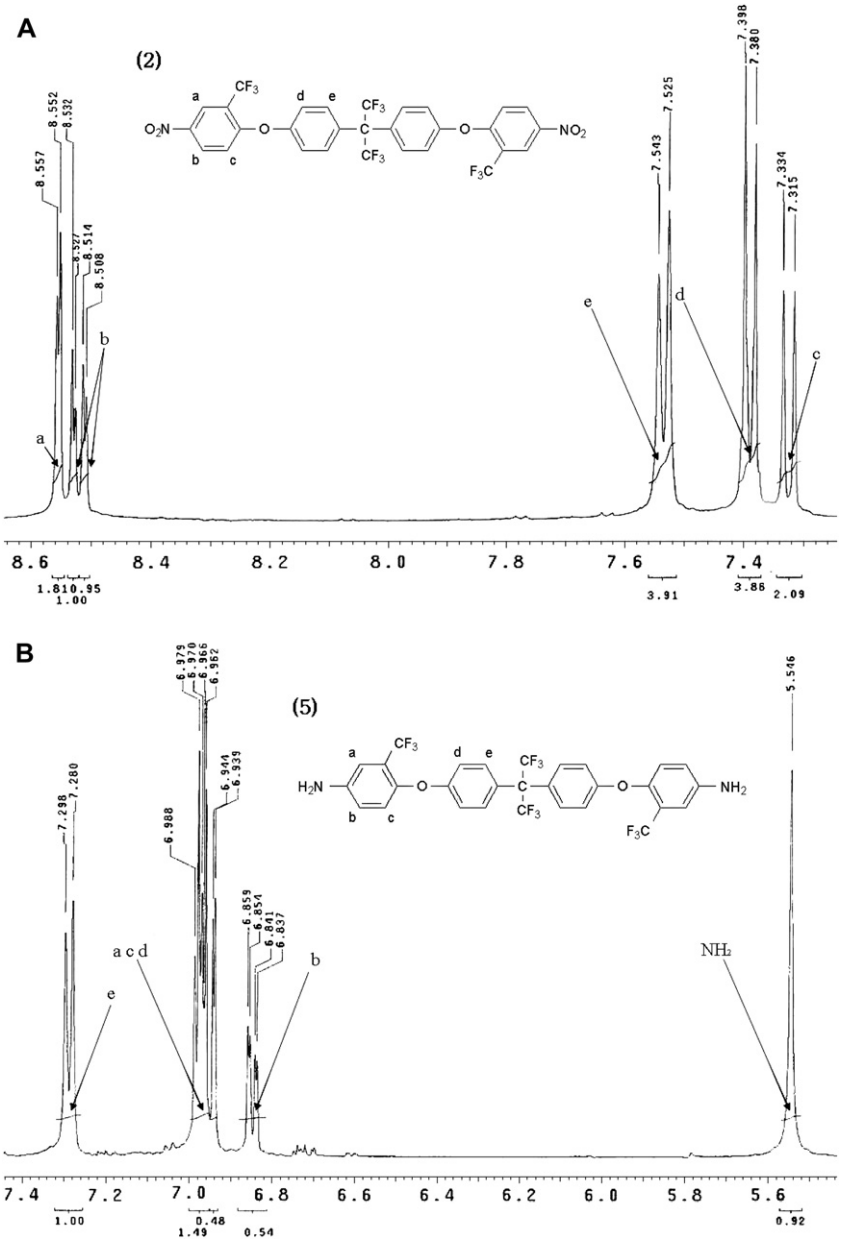

Fig. 3. ^{1}H NMR spectra of (A) dinitro compound (**2**) and (B) diamine (**5**).

8.524 (2H, H_a), 8.518–8.513 (2H, H_b), 7.832, 7.826 (4H, H_e), 7.341, 7.349 (4H, H_d), 7.221, 7.209 (2H, H_c).

2.2.4. 4,4′-Bis(4-amino-2-trifluoromethylphenoxy)diphenyl ether (*4*)

A suspension solution of the purified dinitro compound **1** (0.015 mol) and 10% Pd/C (0.2 g) in methanol and ethyl acetate (volume ratio 1:1) was stirred first for 30 min at room temperature. Then, the mixture was heated up to 60 °C and stirred for another 3 h during the hydrogen gas addition. The reaction solution was filtered to remove Pd/C and the filtrate was concentrated by evaporator, which was dried in vacuum at 80 °C to give a lightly yellow product of **4** (7.06 g, yield: 90.5%).

The T_m is 74 °C by differential scanning calorimetry (DSC) at a scan rate of 10 °C/min. IR (KBr): 3449, 3392 (N–H stretch), 1269 (C–F stretch), 1223, 1187 cm^{-1} (C–O stretch) (Fig. 1). ^{1}H NMR (500 MHz, DMSO): δ (ppm) 7.573, 7.557 (4H, $H_{a,c}$), 6.960–6.924 (8H, H_d), 6.864–6.841 (2H, H_b), 5.505 (4H, NH_2) (Fig. 2).

2.2.5. 2,2-Bis[4-(4-amino-2-trifluoromethylphenoxy)-phenyl]hexafluoropropane (*5*)

A suspension solution of the purified dinitro compound **2** (0.015 mol) and 10% Pd/C (0.25 g) in methanol and ethyl acetate (volume ratio 1:1) was stirred first for 30 min at room temperature. Then, the mixture was heated up to 60 °C and stirred for another 3 h during the hydrogen gas addition. The reaction solution was filtered to remove Pd/C and the filtrate was concentrated by evaporator, which was dried in vacuum at 80 °C to give a lightly yellow product of **5** (8.59 g, yield: 87.5%).

The T_m is 69 °C by differential scanning calorimetry (DSC) at a scan rate of 10 °C/min. IR (KBr): 3440, 3398 (N–H

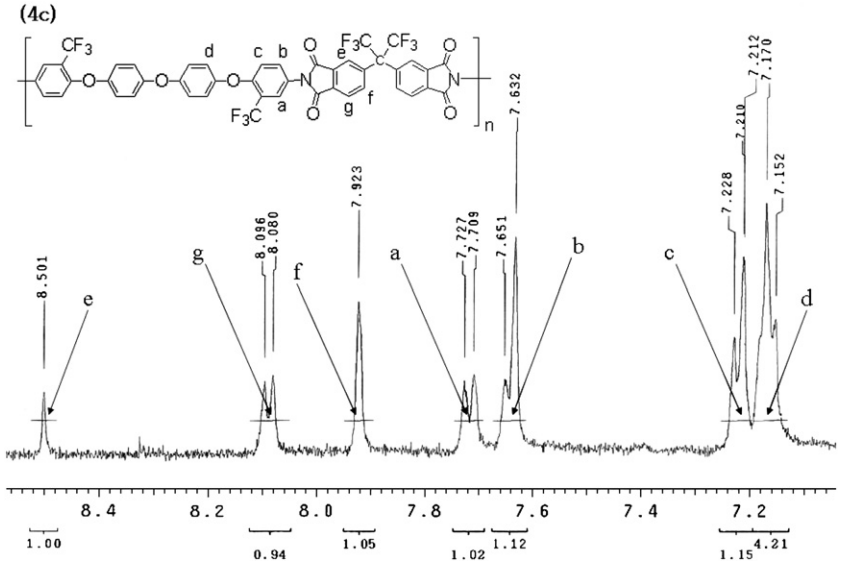

Fig. 4. ^{1}H NMR spectra of polyimide (**4c**).

stretch), 1277 (C−F stretch), 1220, 1179 cm^{-1} (C−O stretch). ^{1}H NMR (500 MHz, DMSO): δ (ppm) 7.298, 7.280 (4H, H_e), 6.980−6.939 (8H, $H_{a,c,d}$), 6.859−6.837 (2H, H_b), 5.546 (4H, NH_2) (Fig. 3).

2.2.6. 4,4′-Bis(4-amino-2-trifluoromethylphenoxy)-diphenyl (*6*)

Similarly, **6** (10.27 g, yield: 91%) was prepared from **3** by the aforementioned procedure.

The T_m is 171 °C by differential scanning calorimetry (DSC) at a scan rate of 10 °C/min. IR (KBr): 3442, 3369 (−NO_2 stretch), 1265 (C−F stretch), 1160, 1126 cm^{-1} (C−O stretch). ^{1}H NMR (500 MHz, DMSO): δ (ppm) 7.548, 7.534 (4H, H_e), 6.951−6.944 (4H, $H_{a,c}$), 6.911, 6.902 (2H, H_d), 6.842−6.839 (2H, H_b), 5.576 (4H, NH_2).

2.3. Synthesis of polyimides

2.3.1. Thermal imidization

Synthesized diamine **4** (3 mmol) was dissolved in 10 mL of dried DMAc in a conical flask under nitrogen gas. After the diamine was dissolved completely, 6FDA (**c**, 3 mmol) was added in one portion. To the stirred mixture, DMAc was added drop by drop depending upon viscosity until total amount of DMAc was 20 mL (15 wt%) in ice bath for 60 min. The mixture was stirred at room temperature for 12 h to form a viscous poly(amic acid) (PAA) solution (**4c**). Then, the obtained PAA solution was spread on a Si wafer, which was placed in an 80 °C oven for 30 min to remove the solvent. The prebaked PAA film was sequentially heated at 120 °C for 10 min, 150 °C for 10 min, 180 °C for 10 min, 210 °C for 10 min, and 250 °C for 30 min. By sonication in water, a flexible PI film of **4c** (T) was self-stripped off the Si wafer.

IR (KBr): 1786, 1731 (asymmetric, symmetric imide C=O stretch), 1377 (C−N stretch), 1098, 721 cm^{-1} (imide ring deformation) and some stronger peak of C−O and C−F stretch was in the range 1100−1300 cm^{-1} (Fig. 1). ^{1}H NMR (500 MHz, DMSO): δ (ppm) 8.501 (2H, H_e), 8.096, 8.080 (2H, H_g), 7.923 (2H, H_f), 7.727, 7.709 (2H, H_a), 7.651, 7.632 (2H, H_b), 7.228−7.212 (2H, H_c), 7.170, 7.152 (8H, H_d) (Fig. 4).

2.3.2. Chemical imidization

The method of synthesis of PAA was similar to the thermal imidization. Then a mixture of acetic anhydride and pyridine (volume ratio 2:1) was added to the PAA solution. The PAA solution was imidized by stirring in oil bath at 110 °C for 6 h, and the obtained solution was spread on a Si wafer, which was spin-coated and placed in an 80 °C oven for 30 min to remove the solvent. And then, the Si wafer was sequentially heated at 120 °C for 10 min, 150 °C for 10 min, 180 °C for 10 min, and 200 °C for 30 min. By sonication in water, a flexible PI film of **4c** (C) was self-stripped off the Si wafer.

Similarly, all other PI films were prepared with the aforementioned procedure.

2.4. Measurements

Fourier transform infrared (FTIR) spectra of the PIs were obtained with a Tensor 27 (Bruker Co.) instrument from 650 to 4000 cm^{-1} on KBr pellets. ^{1}H NMR was analyzed by using Varian Mercury INOVA 500 MHz ^{1}H spectrometer. Differential scanning calorimetric (DSC) analyses were performed on a TA Instruments DSC Q10. Samples of approximately 5−6 mg in weight were sealed in hermetic aluminum pans and scanned in the calorimeter with heating rate of 10 °C/min in the range of 30−300 °C under nitrogen atmosphere, and the melting point (T_m) and glass-transition temperature (T_g) values were taken as the change of the specific heat in the heat flow curves, and peak baseline was determined from the horizontal straight method. For dynamic scanning, calibration of the calorimeter was conducted for the heating rate using an indium standard.

The color intensity of the polymers was evaluated on a HunterLab color QUEST II and a Commission International de 1'Eclairage (CIE)-D illuminant. Measurements were performed

on films of 18–55 μm thick with an observational angle of 10°. A CIE LAB color difference equation was used. Haze data of the polymer films were obtained with Nippon Denshoku 300A Haze meter. Ultraviolet–visible (UV–vis) spectra of the polymer films were recorded on an Agilent UV–visible spectroscopy.

The dielectric properties of PIs are measured by the capacitance method and optical method. The dielectric measurements of PI thin films were monitored at room temperature and 1 kHz with a Fluke PM6304 thin film dielectric analyzer [20]. A sample was placed inside a chamber that isolated the sample from the outside ambient relative humidity and temperature. The capacitance was recorded at room temperature. The dielectric constant (ε') was calculated by the capacitance method from the measured capacitance data as follows:

$$\varepsilon' = \frac{CL}{\varepsilon_0 A}$$

where, C is the capacitance, ε' is the dielectric constant, ε_0 is the permittivity of free space (8.854×10^{-12} F/m), L is the film thickness, and A is the electrode area. For the determination of the dielectric constant by the optical method, the out-of-plane and in-plane refractive indices of the PI thin films were measured with a prism coupler (model 2010, Metricon) equipped with a He–Ne laser light source (wavelength = 632.8 nm) and controlled by a computer. The measurements of the refractive indices were carried out in both transverse electric (TE) and transverse magnetic (TM) modes with the appropriate polarization of the incident laser beam, as described elsewhere [21]. The TE measurement in which the electric field was in the film plane provided the in-plane refractive index, whereas the TM measurement in which the electric field was out-of-plane gave the out-of-plane refractive index.

X-ray Diffractometer (XRD; D/MAX 2500H, Rigaku Co.) was used for measuring morphology of PI thin films. Cu Kα ($\lambda = 1.54$ Å) radiation was used and filtered by monochromator. X-ray generator was run at 40 kV and 50 mA. The sample was multiplied to increase intensity in the range of 3–60° (2θ) at 0.4°/min scan speed and 0.02° intervals.

Thermo gravimetric analysis was done with a thermo gravimetric analyzer (TGA; TA Instruments Co.) from 25 to 800 °C at a heating rate of 10 °C/min in nitrogen atmosphere. The 10 wt% degradation temperature ($T_{10\%}$) and the residues at 800 °C were obtained.

3. Results and discussion

3.1. Monomer synthesis

The fluorinated diamine monomers, **4** and **5**, were prepared through the nucleophilic substitution reaction of 2-chloro-5-nitrobenzotrifluoride with 4,4′-dihydroxydiphenyl ether or 2,2-bis(4-hydroxyphenol)hexafluoropropane in the presence of potassium carbonate, and this was followed by a catalytic reduction with hydrogen gas and Pd/C in ethyl acetate and methanol at 60 °C as shown in Scheme 1.

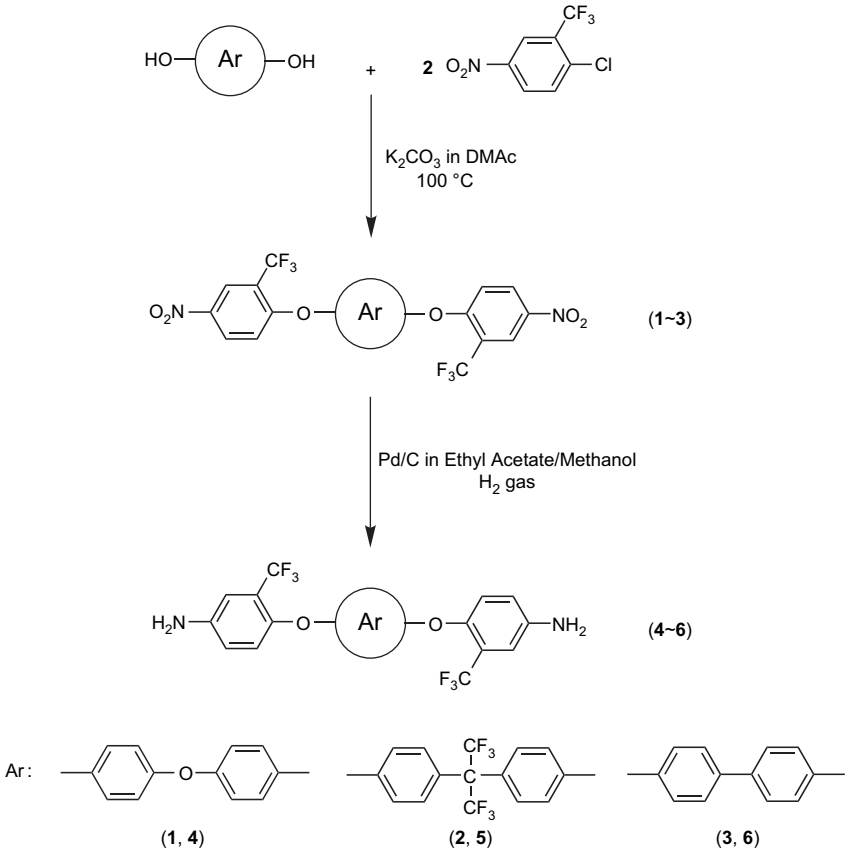

Scheme 1. Synthesis of monomers.

Because the reaction activity of 2-chloro-5-nitrobenzotrifluoride with bisphenol was higher than that of 1-chloro-4-nitrobenzene, both the reaction temperature and the amount of K_2CO_3 could be reduced to avoid coloring of the dinitro compound [22]. In this study, the substitution reaction under 110 °C for 24 h had better results.

The yields in each step were very high, and the obtained products in each step were confirmed by spectroscopic techniques.

FTIR and ^{1}H NMR were used to confirm the structures of the intermediates **1**–**3** and the diamine monomers **4**–**6**. Fig. 1 shows the FTIR spectra of dinitro compound **1** and diamine **4**. The nitro group of compound **1** gave two characteristic bands at 1529 and 1334 cm^{-1} (NO_2 asymmetric and symmetric stretchings). After the reduction, the characteristic absorptions of the nitro group disappeared and the amino group showed a pair of N–H stretching bands in the region of 3300–3500 cm^{-1} (3449, 3392 cm^{-1}). Similarly, absorption bands at 1538 and 1331 cm^{-1} as a result of asymmetric and symmetric stretchings of the NO_2 group of the dinitro compound **2** disappeared after reduction, whereas the characteristic bands of the amino groups at 3440 and 3398 cm^{-1} (N–H stretching) appeared. All of the above compounds exhibited the characteristic absorptions at 1223–1126 cm^{-1} due to ether linkages, and at 1238–1277 cm^{-1} corresponding to CF_3 groups.

Figs. 2 and 3 present the ^{1}H NMR spectra of dinitro compounds **1**, **2** and diamines **4**, **5**. The ^{1}H NMR spectra confirm that the nitro groups were completely converted into amino groups by the high field shift of the aromatic protons. The absorption signals of aromatic protons of **1** appeared in the region of 7.158–8.521 ppm and those of **4** shifted to a higher field between 6.841 and 7.573 ppm. Also, the absorption signals of aromatic protons of **2** appeared in the region of 7.315–8.557 ppm and those of **5** shifted to a higher field between 6.837 and 7.298 ppm. In the ^{1}H NMR spectrums of **1** and **2**, the protons H_a and H_b resonated at the farthest downfield region because of the inductive effect of electron-withdrawing NO_2 and CF_3 groups and the protons H_c and H_d, *ortho*-oriented to aromatic ether, appeared in the upfield region because of the conjugation effect. After the reduction, the protons H_a and H_b of **4** and **5** shifted to the upfield region because of the electron-donating property of the amino groups. The ^{1}H NMR spectra of diamine **5** are similar to those reported [23]. Slightly different chemical shifts of some peaks with respect to the reported values could be attributed to the use of different method of reduction.

These results clearly confirm that the diamines **4** and **5** prepared herein are consistent with the proposed structure.

3.2. Polymer synthesis

The fluorinated PIs of the series **4a**–**6c** were synthesized from diamines **4**–**6** and three different dianhydrides **a**–**c** by a conventional two-step procedure of ring-opening polyaddition at room temperature to form PAA and sequential heating to 250 °C (Thermal imidization, T) or 210 °C (Chemical imidization, C) to obtain the corresponding PIs, as shown in Scheme 2.

For two different approaches, PAA was first produced by the polymerization of diamines **4**–**6** with stoichiometric amounts of three different dianhydrides in DMAc at a solid content of about 15% in ice bath for 12 h, followed by sequential thermal imidization to 250 °C or chemical imidization by adding a

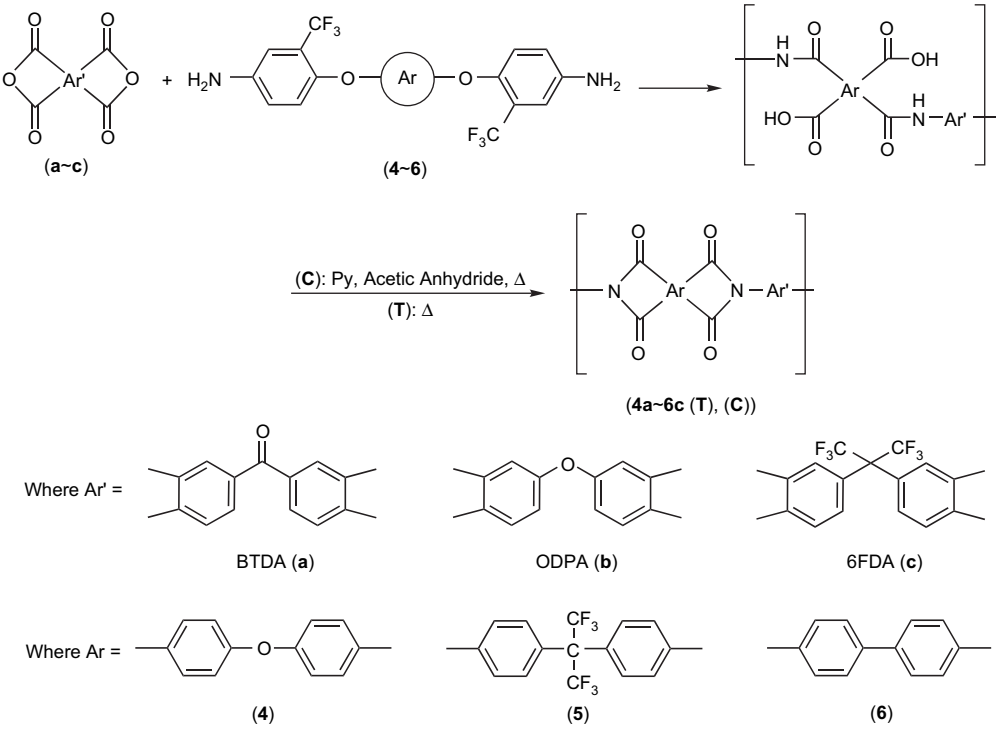

Scheme 2. Synthesis of polyimides.

mixture of acetic anhydride and pyridine (volume ratio 2:1) into the PAA solution at ambient temperature for 30 min followed by heating at 110 °C for 6 h. Transparent, flexible, and strong films were obtained in all cases.

The structures of the PI were characterized by FTIR and ^{1}H NMR spectra. The FTIR spectra of PI **4c** (T) exhibited characteristic imide group absorptions at around 1786 and 1731 cm^{-1} (typical of imide carbonyl asymmetrical and symmetrical stretch), 1377 cm^{-1} (C–N stretch), and 1098 and 721 cm^{-1} (imide ring deformation), together with some strong absorption bands in the region of 1100–1300 cm^{-1} due to the C–O and C–F stretchings (Fig. 1).

The ^{1}H NMR spectra of soluble PI **4c** (T) are shown in Fig. 4. In the ^{1}H NMR spectrum, all the protons resonated in the region of 7.152–8.501 ppm. The proton H_e close to the imide ring appeared at the farthest downfield region of the spectrum because of the resonance. The protons H_c and H_d shifted to a higher field because of the electron-donating property of aromatic ether. The aforementioned results show that series **4** were synthesized successfully.

3.3. Solubility

The solubility of synthesized fluorinated PIs was tested in various organic solvents and the results are summarized in Table 1. The solubility behavior of the PIs depended on their chain packing density and intermolecular interactions. Thus, the PIs derived from more flexible dianhydrides such as **b** and **c** generally displayed a higher solubility than those obtained from more rigid components such as **a**. Series **4**–**6** obtained via thermal and chemical cyclodehydrations were soluble in all test solvents except for **4a** (T), **5a** (T), and **6a** (T). In aprotic polar solvents, such as NMP (*N*-methyl-2-pyrrolidone), DMAc (*N*,*N*-dimethylacetamide), DMF (*N*,*N*-dimethylformamide), and DMSO (dimethyl sulfoxide), they showed excellent solubility and even in less polar solvents, like *m*-cresol, pyridine, THF (tetrahydrofuran), and MC (methylene chloride), they were soluble. This might be due to the presence of the flexible ether structure and the bulky CF_3 substitutes in the diamine, which further hindered dense chain packing and reduced chain–chain interactions. However, the solubility of **a**-based PIs was poorer than most of PIs. This might be attributed to the formation of some intermolecular links of the C=O group of **a** during the thermal imidization [23].

Comparing the solubility of the series **4**–**6**, series **4** and **5** showed better solubility than series **6**. It could be because the diamines with ether group and bulky CF_3 showed great effects, which could inhibit close packing and reduced the interchain interactions to enhance solubility.

Also, the PI prepared by chemical imidization exhibited better solubility than the thermally cured ones. The chemical cyclodehydration method might yield PIs with a less dense packing structure which leads to an improvement in the solubility, whereas the poor solubility of the thermally cured PIs might be attributed comparatively to denser chain packing and aggregation during imidization at elevated temperatures.

3.4. Color intensity and optical transparency

The color intensities of the PIs were explained from the lightness (L^*), yellowness (b^*), and redness (a^*) indices observed with a HunterLab color QUEST II colorimeter. In

Table 1
Solubility behavior of polyimides

Polymer	Solvents[a]								
	NMP	DMAc	DMF	DMSO	*m*-Cresol	Py	THF	MC	Acetone
4a (T)	++	++	+++	++	+	–	++	–	–
4a (C)	+++	++	+++	+++	++	+	++	+	+
4b (T)	+++	++	+++	+++	–	++	+	++	++
4b (C)	+++	++	+++	+++	+	++	++	+++	+++
4c (T)	+++	+++	+++	+++	++	++	+++	+++	+++
4c (C)	+++	+++	+++	+++	+++	+++	+++	+++	+++
5a (T)	++	++	++	++	–	+	–	–	–
5a (C)	++	++	+++	+++	+	+	+	+	+
5b (T)	+++	++	+++	++	+	++	++	++	++
5b (C)	+++	++	+++	+++	++	++	++	+++	+++
5c (T)	+++	+++	+++	++	++	+++	+++	+++	+++
5c (C)	+++	+++	+++	++	+++	+++	+++	+++	+++
6a (T)	+	++	++	++	+	+++	–	–	–
6a (C)	+	++	+++	++	+	+++	+	–	–
6b (T)	+	++	++	++	+	++	+	++	+
6b (C)	+	++	++	++	+	++	++	++	–
6c (T)	+++	+++	++	++	++	+++	++	+++	–
6c (C)	+++	+++	+++	++	++	+++	+++	+++	–

Qualitative solubility was determined with as 10 mg of polymer in 1 mL of solvent. +++: soluble at room temperature; ++: soluble on heating at 100 °C; +: partial soluble on heating; –: insoluble on heating.

[a] NMP, *N*-methyl-2-pyrrolidone; DMAc, *N*,*N*-dimethylacetamide; DMF, *N*,*N*-dimethylformamide; DMSO, dimethyl sulfoxide; Py, pyridine; THF, tetrahydrofuran; MC, methylene chloride.

Table 2
Optical properties of polyimides

Polymer	Film thickness (μm)	Color coordinates[a]			YI[b]	λ_0[c] (nm)	UV-transmittance[d] (%)	Haze[e] (%)
		*b**	*a**	*L**				
4a (T)	22	37.05	−10.17	91.58	42.60	392	85	1.59
4a (C)	18	9.12	−6.05	94.51	13.07	368	91	0.88
4b (T)	25	5.04	−2.52	96.70	6.63	358	92	0.78
4b (C)	32	3.98	−1.96	98.01	3.11	349	94	0.72
4c (T)	23	5.44	−2.30	93.27	2.42	352	93	0.81
4c (C)	18	3.95	−1.36	98.40	1.99	349	94	0.65
5a (T)	18	32.5	−10.6	92.04	39.77	399	89	1.61
5a (C)	21	10.41	−5.56	94.22	11.54	379	89	1.02
5b (T)	27	5.4	−1.88	94.43	5.84	362	96	1.01
5b (C)	28	3.41	−1.42	97.28	3.03	356	93	0.86
5c (T)	24	5.48	−1.92	93.76	2.83	344	95	0.74
5c (C)	28	4.02	−1.18	98.49	1.95	339	95	0.42
6a (T)	27	49.24	−17.21	88.63	65.85	412	72	2.31
6a (C)	55	41.83	−8.81	90.46	31.78	372	76	1.83
6b (T)	39	12.92	−4.96	91.45	12.12	378	78	1.4
6b (C)	34	9.85	−3.11	94.73	9.86	371	84	1.31
6c (T)	45	12.28	−4.81	91.73	11.81	377	80	1.14
6c (C)	45	9.06	−2.79	93.33	8.94	366	89	0.96

[a] The color parameters were calculated according to a CIE LAB equation, with paper as a standard. *L** is lightness; 100 means white and 0 implies black. A positive *a** means red and a negative *a** indicates green. A positive *b** means yellow and a negative *b** indicates blue.
[b] Yellow index (YI) values were measured in conformity with yellowness index of plastics and computing the colors of objects by using the CIE system which were inputted to the computer program into the colorimeter.
[c] Cutoff wavelength defined as the point at which the transmittance becomes less than 1%.
[d] UV-transmittance at 500 nm (%).
[e] Haze (%) values were measured by haze meter. Commonly, an ordinary film's haze value for optical applications would be below haze 5, and an extraordinary film's data would be below haze 3.

this paper, we based our judgment of the degree of yellowness on yellow index (YI) value. The most accurate experiment to measure film's yellowness was a YI authorized by American Standard Test Methods (ASTM) [24,25]. The color coordinates and YI of these PIs are given in Table 2. The results revealed in Table 2 and Fig. 5 indicates that the series **4** and **5** showed not only almost same YI value but also a lower YI value than the corresponding series **6**. Fig. 5 also shows that the color intensity and YI of the PIs were affected by diamine moieties, which decreased in the following order: **6** > **4** > **5**. For various dianhydrides derived PIs, **6a** showed the deepest color, whereas **5c** with four CF_3 groups in the dianhydride moiety exhibited the lightest color. As apparent from Fig. 5, dianhydride structures rather than diamine have significant influence on the YI values.

Thin films were measured for optical transparency with UV–visible spectroscopy. Figs. 6 and 7 show the UV–visible absorption spectra of the PI films prepared via thermal or chemical imidizations, and cutoff wavelength (absorption adge, λ_0) value and the percentage transmittance at 500 nm from these spectra are listed in Table 2. In agreement with the results obtained from the colorimeter, all PI series **4** and

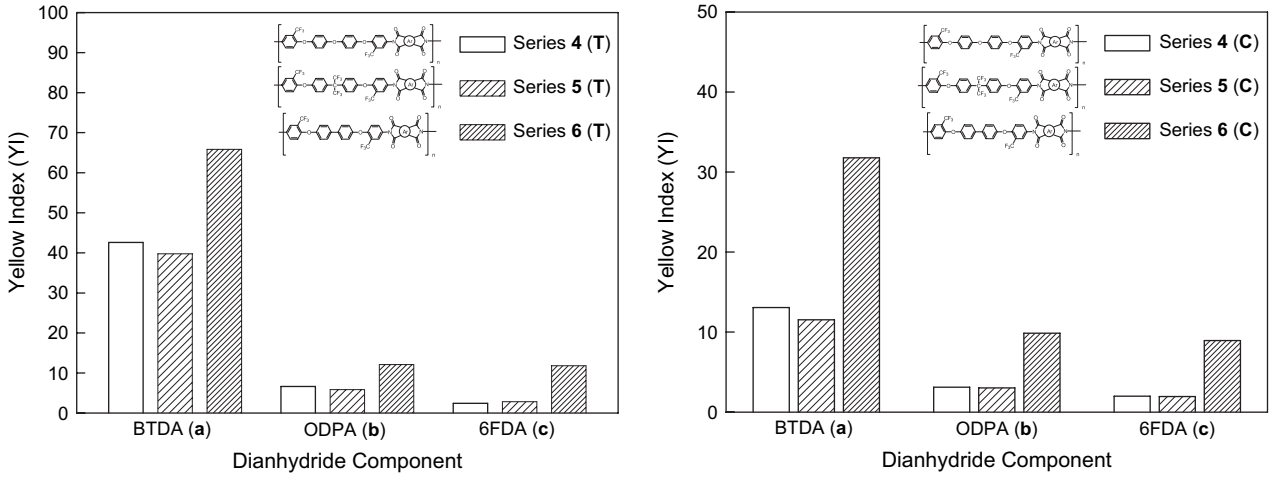

Fig. 5. Comparison of YI values for polyimide series (**4**–**6**).

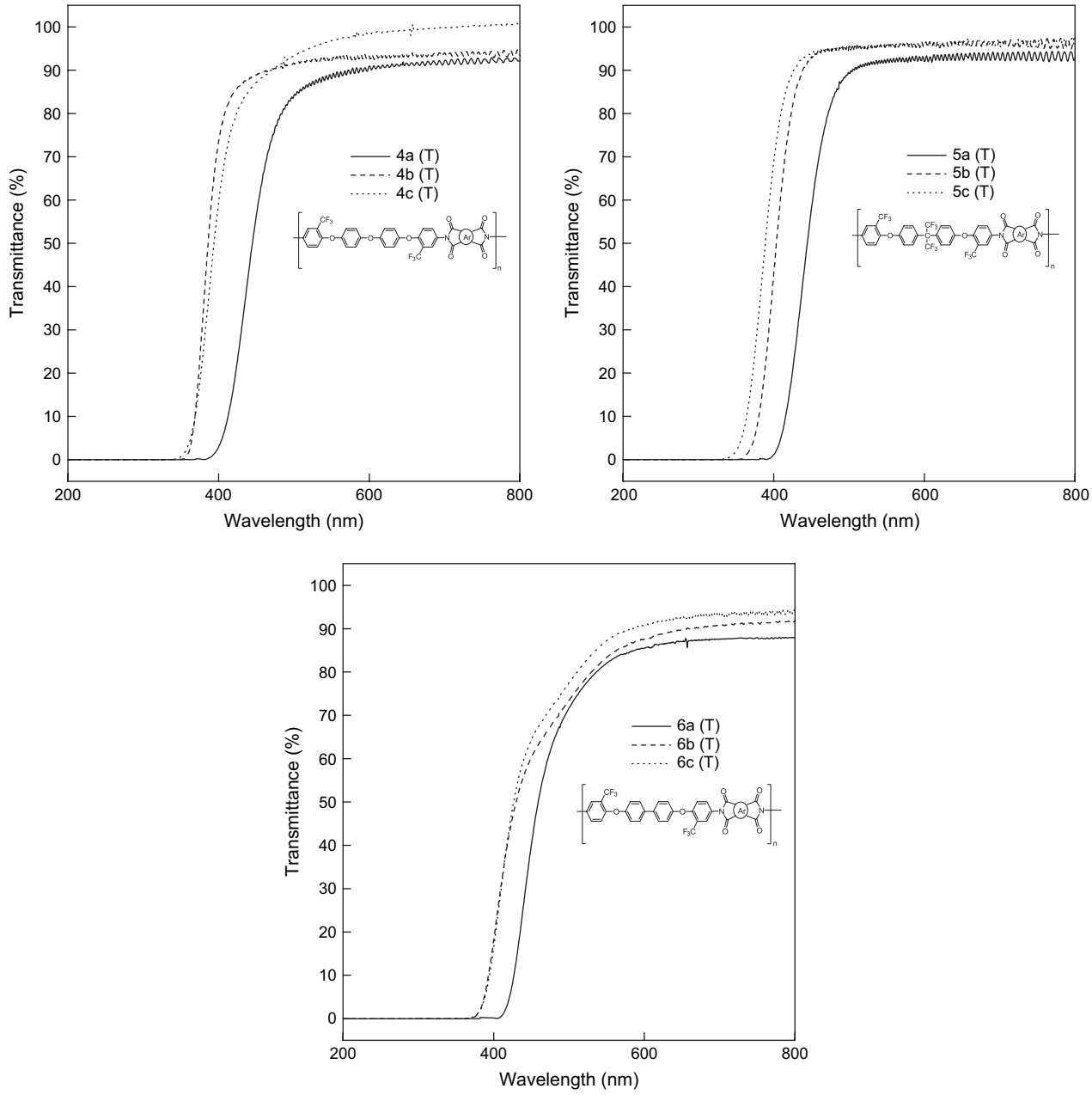

Fig. 6. UV–visible spectra of thermally imidized polyimides.

5 revealed a shorter λ_0 than their respective analogue series **6**. Except for **a**-based PIs, the other fluorinated PIs had shorter λ_0 than 400 nm, and all the PI series **4** and **5** exhibited high optical transparency of 85–95%.

As a result, all the fluorinated PIs which have flexible group like ether linkage or bulky CF_3 group in the center of diamine chain optically advanced by contrast with the corresponding comparatively rigid diamine **6**-based ones. In addition, each PIs produced from **b** and **c** were fairly transparent and almost colorless in contrast to other dianhydride, **a**. These results were attributed to the reduction of the intermolecular CTC between alternating electron-donor (diamine) and electron-acceptor (dianhydride) moieties. The ether chain of diamine **4** or **b** and the CF_3 group of diamine **5** or **c** could inhibit the formation of the CTC. The light colors of the PIs with the CF_3 groups in their diamine moieties could be explained from the decreased intermolecular interactions. The bulky and electron-withdrawing CF_3 group was effective in reducing the CTC formation between polymer chains through steric hindrance and the inductive effect (by decreasing the electron-donating property of the diamine moieties). Moreover, the CF_3 group might weaken chain-to-chain cohesive force due to lower polarizability of the C–F bond. The decrease in intermolecular CTC formation is understandable also from the significant solubility of the PIs prepared from diamine. Consistent with the effect of CF_3 group, the flexible ether

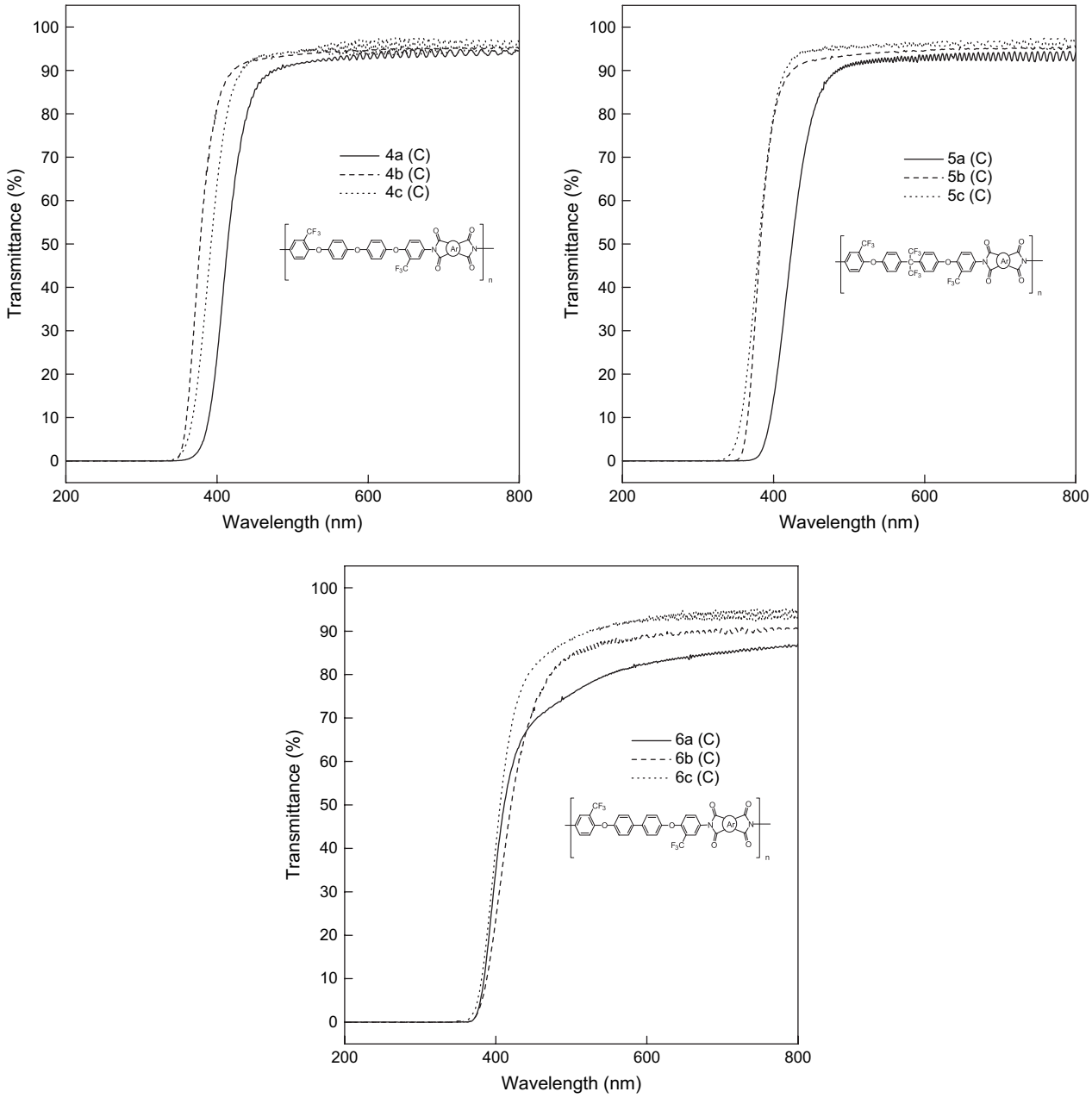

Fig. 7. UV–visible spectra of chemically imidized polyimides.

group was also sufficiently effective in reducing CTC formation.

On comparing thermal imidization polymers with chemical imidized ones, chemical imidized ones showed a lower YI values than thermal imidized ones. Including the results of UV–visible spectra, chemical imidized PIs were more transparent than thermal imidized ones. It may be expected that the chain intermolecular distance after imidization by thermal and chemical methods attributed to YI values would be explained by morphological structures.

For the all fluorinated PIs, haze values showed small differences below haze 3, which means synthesized PIs were clean and no turbidity.

3.5. Thermal properties

DSC and TGA were used to evaluate the thermal properties of the PI films. The thermal behavior data of all the fluorinated PIs are given in Table 3. The glass-transition temperature (T_g) values of the PIs were obtained from DSC and DMA measurements. PI series **4** and **5** showed T_g values in the ranges of 229–249 and 221–243 °C, respectively. When the two series of PIs were compared, the PI series **4** generally revealed slightly higher T_g values than their series **5** counterparts. This could be attributed to high free volume present in series **5**, due to bulky CF_3 moieties and non-coplanarity of diamine **5** when compared to diamine **4**.

Table 3
Thermal properties of polyimides

Polymer	DSC	TGA	
	T_g[a] (°C)	$T_{10\%}$[b] (°C)	Char yield[c] (%)
4a (T)	240	568	56.6
4a (C)	238	560	52.7
4b (T)	232	590	55.8
4b (C)	229	569	53.4
4c (T)	249	540	52.6
4c (C)	243	530	48.5
5a (T)	244	558	52.8
5a (C)	230	557	49.3
5b (T)	227	569	53.2
5b (C)	221	552	51.7
5c (T)	243	543	50.8
5c (C)	240	530	48.8
6a (T)	257	596	60.5
6a (C)	249	585	58.9
6b (T)	248	600	60.6
6b (C)	239	595	58.9
6c (T)	268	567	52.9
6c (C)	260	569	51.9

[a] Baseline shift in the second heating DSC traces, with a heating rate of 10 °C/min.
[b] Temperature at 10% weight loss.
[c] Residual weight (%) when heated to 800 °C.

But, depending on the dianhydride component, the PI obtained from **b** showed the lowest T_g and PI derived from **c** had the highest T_g in each series. This might be a result of higher steric hindrance of segmental mobility caused by the CF_3 groups, although they might result in higher free volume and weaken the interchain interactions, which should reduce T_g. On the other hand, PI series **6** showed higher T_g values (239–268 °C) than those of structurally similar fluorinated PIs. This could be explained in terms of an increased formation of crystallinity due to the removal of the functional groups.

The thermal stabilities of these PIs were evaluated by TGA under nitrogen with a 10% weight-loss temperature ($T_{10\%}$) for comparison. These are summarized in Table 3. The decomposition temperatures at a 10% weight loss of PIs **4a**–**4c** were recorded in the range of 530–590 °C in nitrogen and those of PIs **5a**–**5c** were recorded in the range of 530–569 °C. Most of the fluorinated PIs **6a**–**6c** exhibited higher $T_{10\%}$ values than their analogous **4** and **5** counterparts and this increase may be a result of relatively higher rigidity of the molecular chains.

All the PIs left more than 48.5% char yields at 800 °C in nitrogen. The TGA results showed an excellent thermal stability of these PIs, even though they revealed high solubility and optical transparency. In addition, the thermal stability of PI series **4** was slightly higher than that of PI series **5** and **c**-based PIs showed the lowest thermal stability when compared the types of dianhydride. This can be attributed to the presence of unstable CF_3 groups. In hexafluoroisopropylidene group containing polymer, it does not have the conformational freedom since the bulky CF_3 groups retard free rotation even on their own axis thus giving rise to high torsional strain. Higher steric and conformational energies can be released by the loss of CF_3 groups. This leads to easy dissociation of CF_3 radicals [26]. Hence, PIs with CF_3 groups exhibited high T_g but low thermal decomposition.

3.6. Dielectric constants

The dielectric constants for the PI thin films were evaluated by capacitance method (2.74–3.44) and optical method (2.59–2.93), respectively, and the values are summarized in Table 4 and Fig. 8. The dielectric constants measured by capacitance method (ε_{cap}) were measured at 1 kHz, and also measured by optical method (ε_{opt}) using Maxwell relation that was calculated from the refractive index of PI thin films in the transverse electric (TE) and transverse magnetic (TM) modes which were obtained from prism coupler. An average index (n_{av}) was calculated with the equation $n_{av} = (2n_{TE} + n_{TM})/3$ and its birefringence (Δn) is given as the difference between n_{TE} and n_{TM}. The dielectric constant (ε_{opt}) of the materials at optical frequencies can be estimated from the refractive index (n_{av}) according to Maxwell's equation, $\varepsilon_{opt} \approx n^2$. ε_{opt} at around 1 MHz is evaluated to be $\varepsilon_{opt} \approx 1.1\ n^2$, including an additional contribution of approximately 10% from the IR absorption [27]. For comparison with dielectric properties, the dielectric constant by optical method was taken in the perpendicular direction of the film orientation. A similar trend of variation in dielectric constants by the capacitance and optical methods was obtained, but the dielectric constants by capacitance method were higher than values by optical method in all the cases. In the capacitance method, the electronic and nuclear polarizabilities contribute to the overall dielectric constant, whereas in the optical method the electronic polarizability contributes. Hence the dielectric constants obtained by the

Table 4
Dielectric constants of polyimides

Polymer	Capacitance method	Optical method				
	ε_{cap} (1 kHz)	n_{TE}[a]	n_{TM}[b]	n_{av}[c]	Δn[d]	ε_{opt}[e] (1 MHz)
4a (T)	3.44	1.6340	1.6311	1.6330	0.0029	2.9334
4a (C)	3.30	1.6142	1.5978	1.6087	0.0164	2.8467
4b (T)	3.29	1.6078	1.6020	1.6059	0.0058	2.8368
4b (C)	3.15	1.6033	1.5979	1.6015	0.0054	2.8213
4c (T)	2.91	1.5688	1.5541	1.5639	0.0147	2.6904
4c (C)	2.83	1.5590	1.5451	1.5544	0.0139	2.6578
5a (T)	3.28	1.6021	1.5944	1.5995	0.0029	2.8142
5a (C)	3.19	1.5942	1.5768	1.5884	0.164	2.7753
5b (T)	3.21	1.5878	1.5820	1.5859	0.0058	2.7666
5b (C)	3.05	1.5773	1.5679	1.5742	0.0054	2.7259
5c (T)	2.89	1.5419	1.5301	1.5380	0.0147	2.6019
5c (C)	2.74	1.5380	1.5251	1.5337	0.0139	2.5875

[a] In-plane refractive index at 632 nm: n_{TE}.
[b] Out-of-plane refractive index at 632 nm: n_{TM}.
[c] Average refractive index $n_{av} = (2n_{TE} + n_{TM})/3$.
[d] Birefringence $\Delta n = n_{TE} - n_{TM}$.
[e] Dielectric constant estimated from the refractive index at 632 nm: $\varepsilon_{opt} = 1.10 n_{av}^2$.

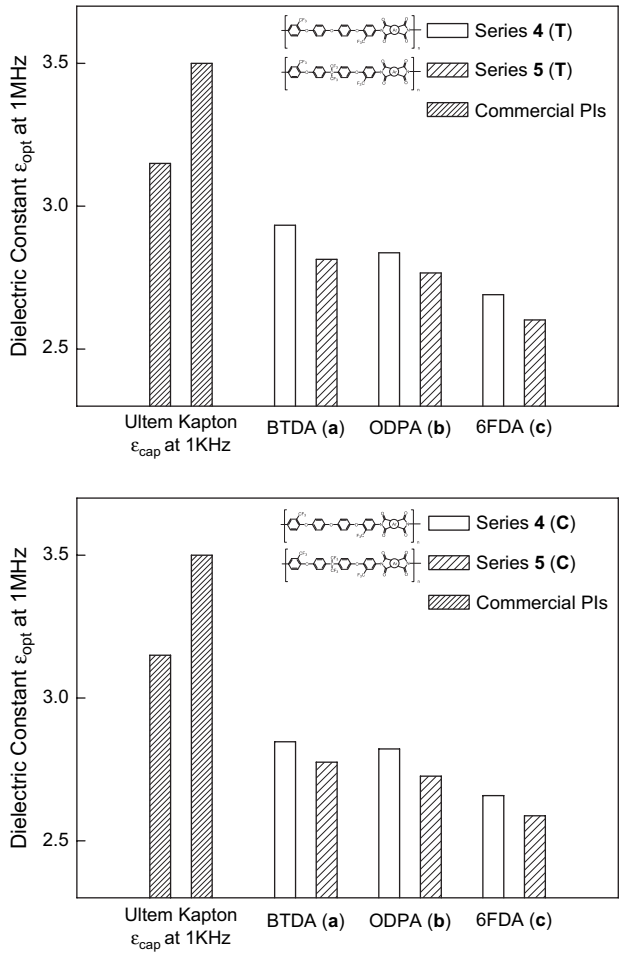

Fig. 8. Comparison of dielectric constants for polyimide series (**4**) and (**5**).

capacitance method are always higher than values obtained by the optical method [28,29].

PIs **5a**–**5c** had lower dielectric constants (2.59–2.81 at 1 MHz) than PIs **4a**–**4c** (2.66–2.93 at 1 MHz). The decreased dielectric constants might be attributed to the presence of bulky CF_3 groups in the center of diamine structure, which brought about less efficient chain packing and an increased free volume. In addition, the strong electronegativity of fluorine resulted in very low polarizability of the CF bonds, reducing the dielectric constant. The PI series **4** and **5** had different dielectric constant, but on the other hand all fluorinated PIs had lower dielectric constants than commercial PIs such as Kapton films ($\varepsilon_{cap} = 3.5$ at 1 kHz) and Ultem ($\varepsilon_{cap} = 3.15$ at 1 kHz) [30].

Considering the type of dianhydride backbone, the dielectric constant from both capacitance and optical methods lists in the following order: **c** < **b** < **a**. PIs having **c** exhibited lowest dielectric constants because of presence of bulky CF_3 groups. When **a** and **b** were considered, **a** having carbonyl bridge (C═O) has less free volume than the oxygen bridge (–O–) of **b** and C═O imparts more polarizability and moisture absorption in the PI backbone when compared to the –O– bridge resulting in higher dielectric constant.

3.7. Morphological structure

The morphological structure of the PI films was analyzed by Wide-Angle X-ray Diffraction (WAXD). All the PI films exhibited amorphous halo whose featureless lattice existed in the main chain. (Figs. 9 and 10) This was reasonable because the PIs contained laterally attached, non-coplanar unit of diamine that sterically disrupted the chain packing and inhibited significant chain–chain interactions. The amorphous nature of the PI series **4**–**6** could be attributed in part to the presence of the bulky CF_3 groups, which resulted in a less dense chain packing structure. Therefore amorphous halo represents PI chain packed unsystematically. As expected this trend not only showed in flexible dianhydride based PI like **c** and **b** but also represented in comparatively rigid dianhydride **a** because all PIs contained fluorinated diamine **4**–**6** in the backbone. Specially, the mean intermolecular distances calculated from the peak maximum of the reflection WAXD patterns for **4c** (T) and **4c** (C) in Fig. 9 were 4.4140 Å (20.10°) and 5.2574 Å (16.85°), respectively. It is a good agreement with a reason why the YI of the polyimide film synthesized with chemical imidization is different from that of them with thermal imidization in Table 2.

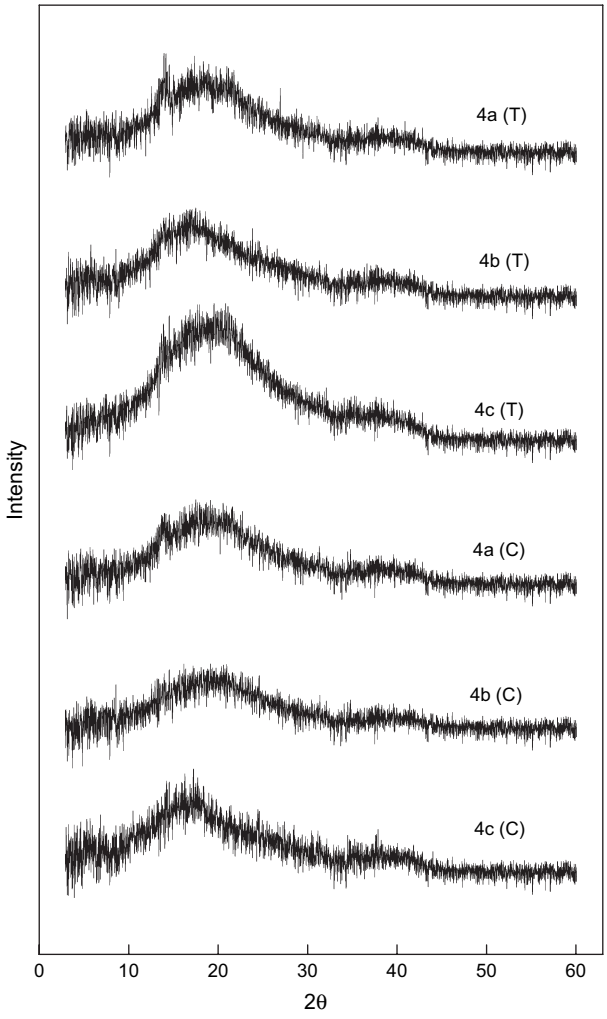

Fig. 9. WAXD patterns of polyimide series (**4**).

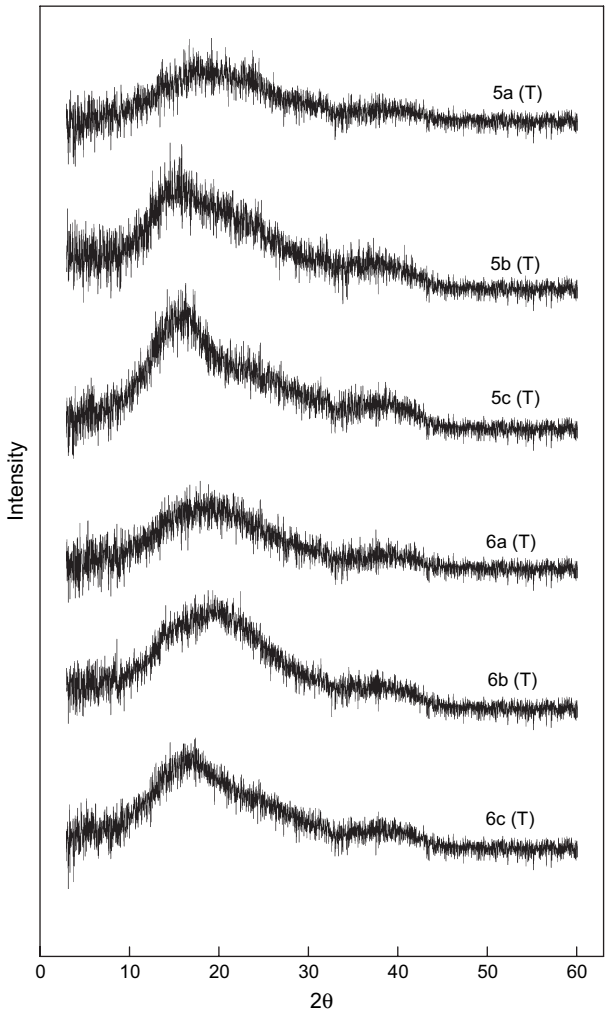

Fig. 10. WAXD patterns of polyimide series (**5**) and (**6**).

4. Conclusions

Fluorinated diamines, **1**–**3**, were synthesized via a high yielding two-step procedure. Three series of designed organo-soluble and colorless fluorinated PIs, **4a**–**6c**, were obtained successfully from **1**–**3** with various aromatic dianhydrides by two different thermal and chemical imidization methods. The obtained PIs displayed excellent solubility, fantastic optical properties, high thermal stability, good mechanical property and lower dielectric constant. Especially, we compared PI series **4** with PI series **5** to investigate the difference of the CF_3 group and ether group affecting the optical property of PIs. As a result, we confirmed that both PI series **4** and **5** showed light color and great transparence that is nearly equal to the colorless PI, but PI series **4** was slightly more colorless than PI series **5**. In addition, PI series **4** exhibited better thermal stability than PI series **5**. These PIs may be the most promising, processable high-temperature materials for applications in microelectronic and optical devices.

Acknowledgement

This work was supported by the Korean Science and Engineering Foundation through the National Research Laboratory Program.

References

[1] Matsumoto T. Recent Res Dev Polym Sci 1999;3:405.
[2] Feger C, Khojasteh MM, McGrath JE. Polyimides: materials, chemistry and characterization. Amsterdam: Elsevier; 1989.
[3] Tamai S; Ohta M; Kawashima S; Oikawa H; Ohkoshi K; Yamaguchi A. Eur Patent 234, 882; 1987.
[4] Ando S, Sawada T, Inoue Y. Electron Lett 1993;29:2143.
[5] Hergenrother PM, Havens SJ. Macromolecules 1994;27:4659.
[6] Chern YT. Macromolecules 1998;31:5837.
[7] Hasio SH, Yang CP, Yang CY. J Polym Sci Part A Polym Chem 1997;35:1487.
[8] Reddy DS, Chou CF, Shu L, Gh L. Polymer 2003;44:557.
[9] Yang CY, Yang HW. J Appl Polym Sci 2000;75:87.
[10] Yin DX, Li YF, Yang SY, Fan L, Liu JG. Polymer 2005;46:3119.
[11] Yang CP, Chen RS. J Polym Sci Part A Polym Chem 2000;38:2082.
[12] Yang CP, Su YY. Polymer 2003;44:6311.
[13] Qu W, Ko TM, Vora RH, Chung TS. Polymer 2001;42:6393.
[14] Yang CP; Yang HW. US Patent 6,093,790; 2000.
[15] Rogers FE. US Patent 3,356,648; 1964.
[16] Dine-Hart RA, Wright WW. Macromol Chem 1971;143:189.
[17] Liaw DJ, Liaw BY. Macromol Chem Phys 1998;199:1473.
[18] Wang CS, Yang RW. J Appl Polym Sci 1997;66:609.
[19] Yang CP, Chen RS, Chen CP. J Polym Sci Part A Polym Chem 2003;41:922.
[20] Chung HS, Joe YI, Han HS. Polym J 1999;31:700.
[21] Chung HS, Joe YI, Han HS. J Appl Polym Sci 1999;74:3287.
[22] Wang CP, Chen RS, Chen KH. J Appl Polym Sci 2005;95:922.
[23] Yang CP, Chen RS, Hsu MF. J Polym Res 2002;9:245.
[24] AK St Clair; TL St Clair. US Patent 4,603,061; 1986.
[25] AK St Clair; TL St Clair. US Patent 4,595,548; 1986.
[26] Hougham G, Cassidy PE, John K, Davidson T. Fluoropolymers 2: properties. New York: Kluwer Academic/Plenum; 1999. p. 233.
[27] Watanabe Y, Shibasaki Y, Ando S, Ueda M. J Polym Sci Part A Polym Chem 2004;42:144.
[28] Lee CK, Shul YG, Han HS. J Polym Sci Part B Polym Phys 2002;40:2190.
[29] Lin CH, Jiang ZR, Wang CS. J Polym Sci Part A Polym Chem 2002;40:4084.
[30] Banerjee S, Madhra MK, Kute V. J Appl Polym Sci 2004;93:821.